

Structure and property of a vertical cutting $\text{Ca}_{0.4}\text{Sr}_{0.6}\text{Bi}_4\text{Ti}_4\text{O}_{15}$ ferroelectric ceramic

Su-Hua Fan*, Ran Yu, Feng-Qing Zhang, Quan-De Che and Wei Hu

School of Material Science and Engineering, Shandong Jianzhu University, Jinan 250101, China

$\text{Ca}_{0.4}\text{Sr}_{0.6}\text{Bi}_4\text{Ti}_4\text{O}_{15}$ ceramics with a -axis preferred orientation were prepared by a solid-state reaction method. The cylindrical $\text{Ca}_{0.4}\text{Sr}_{0.6}\text{Bi}_4\text{Ti}_4\text{O}_{15}$ ceramics were cut into two types of plates: one was along the cylinder axis (A), and the other was perpendicular to the direction of the cylinder axis. The effects of sintering temperature on the structure and electrical properties of the $\text{Ca}_{0.4}\text{Sr}_{0.6}\text{Bi}_4\text{Ti}_4\text{O}_{15}$ ceramics were investigated. When the sintering temperature was 1180 °C, sample A gave the highest a -axis (200) orientation with a value of about 27.1%. At this sintering temperature, sample A showed better dielectric properties and ferroelectric properties, the relative dielectric constant (ε_r), dielectric loss ($\tan \delta$), remnant polarization (P_r), and coercive field (E_c) were 217.6, 0.0027, 14.2 $\mu\text{C}/\text{cm}^2$ and 49.6 kV/cm, respectively.

Key words: $\text{Ca}_{0.4}\text{Sr}_{0.6}\text{Bi}_4\text{Ti}_4\text{O}_{15}$ ceramic, grain orientation, ferroelectric property.

Introduction

Bismuth-layer-structured ferroelectrics (BLSFs) are attractive materials because of their potential application in ferroelectric random access memories (FeRAMs). The general chemical formula of BLSFs is $(\text{B}_2\text{O}_2)^{2+}(\text{A}_{m-1}\text{B}_m\text{O}_{3m+1})^{2-}$, where A is a mono-, di- or trivalent element, with dodecahedral coordination, B is a transition cation suited to dodecahedral coordination, and m is an integer, which represents the number of perovskite layers. Their structure can be regarded as a regular intergrowth of $(\text{B}_2\text{O}_2)^{2+}$ layers and $(\text{A}_{m-1}\text{B}_m\text{O}_{3m+1})^{2-}$ perovskite-like slabs [1-2]. As a typical member of the BLSFs, $\text{SrBi}_4\text{Ti}_4\text{O}_{15}$ (SBTi) consists of four TiO_6 octahedra in perovskite blocks sandwiched by two neighboring $(\text{Bi}_2\text{O}_2)^{2+}$ layers along the c -axis in a unit cell. Its relatively high Curie temperature ($T_c = 520$ °C) makes it applicable over a wide temperature range [3-4]. It has been reported that $2P_r$ in SBTi single crystal is 58 $\mu\text{C}/\text{cm}^2$ along the a -axis under an applied electric field of 60 kV/cm [5]. $\text{CaBi}_4\text{Ti}_4\text{O}_{15}$ (CBTi) is characterized by its high T_c of about 790 °C and therefore is expected to be useful for special applications at relatively higher temperatures [6]. Since SBTi has the same structure as that of CBTi, one can expect that Ca^{2+} doping could improve the ferroelectricity of SBTi. In previous studies, ferroelectricity was observed in the $\text{Ca}_{0.4}\text{Sr}_{0.6}\text{Bi}_4\text{Ti}_4\text{O}_{15}$ ceramics. The results showed that the P_r and E_c of $\text{Ca}_{0.4}\text{Sr}_{0.6}\text{Bi}_4\text{Ti}_4\text{O}_{15}$ ceramic were 8.37 $\mu\text{C}/\text{cm}^2$ and 72 kV/cm, respectively [7]. Mao *et al* [8-9] have cut $\text{Bi}_4\text{Ti}_3\text{O}_{12}$ ceramics parallel and perpendicular to the direction of the cylinder axis. It was found that the remnant polarization of the parallel cut sample ($2P_r = 41.2 \mu\text{C}/\text{cm}^2$) was larger than

the perpendicular cut sample ($2P_r = 5.8 \mu\text{C}/\text{cm}^2$), because the parallel cut sample showed preferred a -axis orientation.

In the present study, $\text{Ca}_{0.4}\text{Sr}_{0.6}\text{Bi}_4\text{Ti}_4\text{O}_{15}$ ferroelectric ceramics were prepared by a solid-state reaction method. The ceramics were cut into two types along and perpendicular to the cylinder axis. The effects of the cutting direction and sintering temperature on the structure and electrical properties of the $\text{Ca}_{0.4}\text{Sr}_{0.6}\text{Bi}_4\text{Ti}_4\text{O}_{15}$ ceramics were investigated.

Experimental Procedure

The $\text{Ca}_{0.4}\text{Sr}_{0.6}\text{Bi}_4\text{Ti}_4\text{O}_{15}$ ceramics were prepared by a solid-state reaction method. All reagents used were analytically pure. Calcium carbonate (CaCO_3), strontium titanate (SrCO_3), titanium dioxide (TiO_2), and bismuth oxide (Bi_2O_3) powders were mixed for 15 h using a ball milling process in distilled water. 10% (in mass) excess bismuth was added to compensate for the bismuth loss during the sintering process. The mixed powders were preheated at 600 °C for 1 h and pressed into disks with a size of 15 mm × 8 mm. Then the disks were sintered in the temperature range of 1100-1210 °C for 2 h. The cylindrical $\text{Ca}_{0.4}\text{Sr}_{0.6}\text{Bi}_4\text{Ti}_4\text{O}_{15}$ ceramics were cut into two types of plates shown in Fig. 1

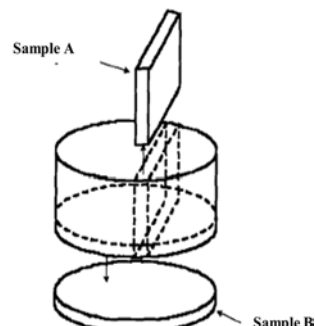


Fig. 1. Sketch map of the samples.

*Corresponding author:

Tel : +0531-86526688

Fax: +0531-86526786

E-mail: fsuhua@126.com

[8]. One was along the cylinder axis (sample A), and the other was perpendicular to the direction of the cylinder axis (sample B).

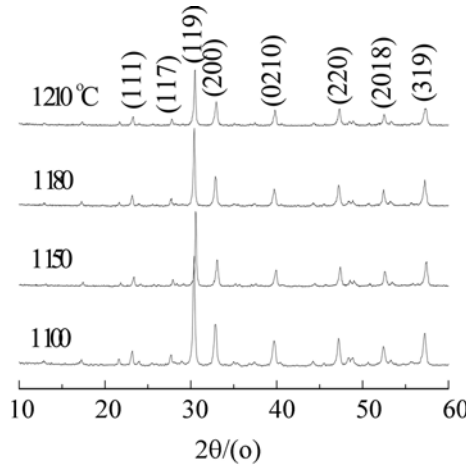
The crystallization characteristics and orientation behavior of the $\text{Ca}_{0.4}\text{Sr}_{0.6}\text{Bi}_4\text{Ti}_4\text{O}_{15}$ ceramics were analyzed using X-ray diffraction (XRD). The microstructure of $\text{Ca}_{0.4}\text{Sr}_{0.6}\text{Bi}_4\text{Ti}_4\text{O}_{15}$ ceramic was observed by a scanning electron microscope (SEM, model Sirion 200, FEI). The dielectric permittivity of the samples was measured using an impedance analyzer (model HP4294A). The room temperature ferroelectric property was measured by a radiant precision workstation.

Results and Discussion

The XRD patterns of the $\text{Ca}_{0.4}\text{Sr}_{0.6}\text{Bi}_4\text{Ti}_4\text{O}_{15}$ ceramics are shown in Fig. 2. Although 10% of extra bismuth was added, no secondary phase can be found, indicating that a pure $\text{Ca}_{0.4}\text{Sr}_{0.6}\text{Bi}_4\text{Ti}_4\text{O}_{15}$ perovskite phase was obtained in all samples. Compared with the XRD patterns of sample B, the intensity of the (200) peak of sample A was stronger and the intensities of the (001) peak were very weak and even disappeared, while the intensities of the (001) peak of sample B were predominant. The difference in crystallization behavior of the samples parallel and perpendicular to the cutting direction may be attributed to the effects of the axial compression and highly anisotropic properties of the Bi-layered perovskite structure [8-9], which is further studied.

In order to evaluate the effects of the grains with different orientations on the electrical properties, the volume fractions for the main diffraction peaks were calculated based on Ref [10], which are shown in Table 1.

$$\left. \begin{aligned} \alpha_{(100)} &= (I_{(100)}/I^*_{(100)})/\sum(I_{(hkl)}/I^*_{(jkl)}) \\ \alpha_{(119)} &= (I_{(119)}/I^*_{(119)})/\sum(I_{(hkl)}/I^*_{(jkl)}) \\ \alpha_{(001)} &= (I_{(001)}/I^*_{(001)})/\sum(I_{(hkl)}/I^*_{(jkl)}) \end{aligned} \right\} \quad (1) [10]$$



(a) Samples A

Table 1. Volume fractions and its ratio to the main diffraction peak of $\text{Ca}_{0.4}\text{Sr}_{0.6}\text{Bi}_4\text{Ti}_4\text{O}_{15}$ ceramics sintered at different temperatures.

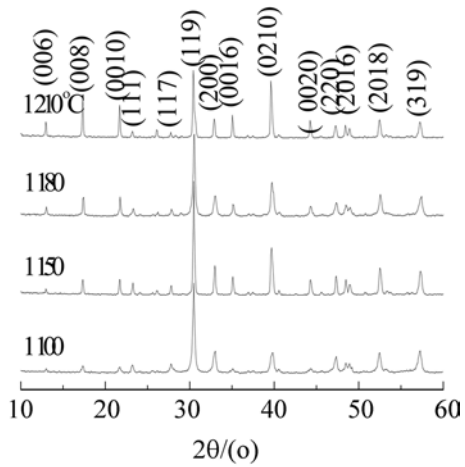
Temperature/ °C	$\alpha_{(200)}/\%$									
	A	B	A	B	A	B	A	B	A	B
1100	25.3	18.1	24.2	24.5	21.0	25.8	30.4	31.6	1.05	0.74
1150	25.5	7.9	23.5	9.2	18.6	39.8	29.8	26.1	1.09	0.86
1180	27.1	20.6	21.0	18.0	19.8	30.7	31.6	30.7	1.29	1.14
1210	25.7	11.9	23.0	15.4	20.0	44.0	27.9	28.6	1.18	0.77

A—sample A; B—Sample B.

where α means the volume percent, (hkl) means crystal face indices, $I_{(hkl)}$ and $I^*_{(jkl)}$ means the relative intensity of the diffraction peak of the ceramic and powder.

It can be seen from Table 1 that the relative intensity of the (200) peak initially increased with an increase of the sintering temperature from 1100 °C to 1180 °C, and the (200) peak became predominant at 1180 °C, indicating that the grains with a -axis orientation were enhanced. In addition, the largest α (200) values of the sample A and the sample B were α (200) = 27.1% and α (200) = 20.6%, respectively. It is generally known that the ferroelectric properties of the BLSFs are affected by the anisotropies of the a - and b -axes rather than that of the c -axis [11]. Therefore, it could be anticipated that sample A would have better ferroelectricity than sample B. Since the major polarization vector of this family is close to the a -axis orientation, it is favorable for the ferroelectric properties of the sample A.

The bulk densities of sample A measured by Archimedes method are shown in Fig. 3. It can be seen that the bulk density of the sample A drastically increased from 5.81 g/cm³ to 7.24 g/cm³ with the sintering temperature changed from 1100 °C to 1180 °C. When the sintering temperature reached 1210 °C, the bulk density of sample A decreased (ρ = 6.17 g/cm³), which can be ascribed to the effects of the pores formed caused by the loss of bismuth and the formation



(b) Sample B

Fig. 2. XRD patterns of samples A and B sintered at different temperatures.

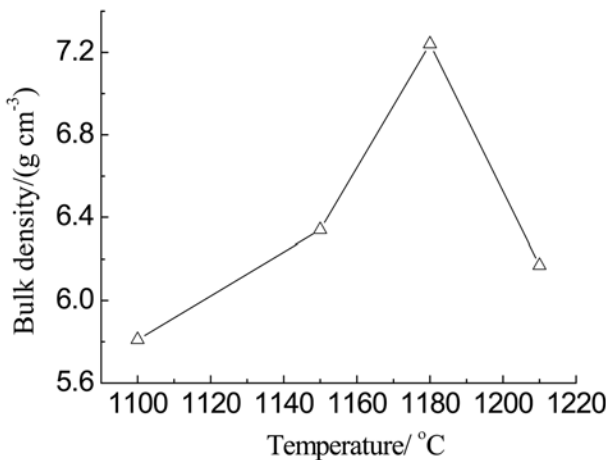


Fig. 3. Bulk density of sample A sintered at various temperatures for 2 h.

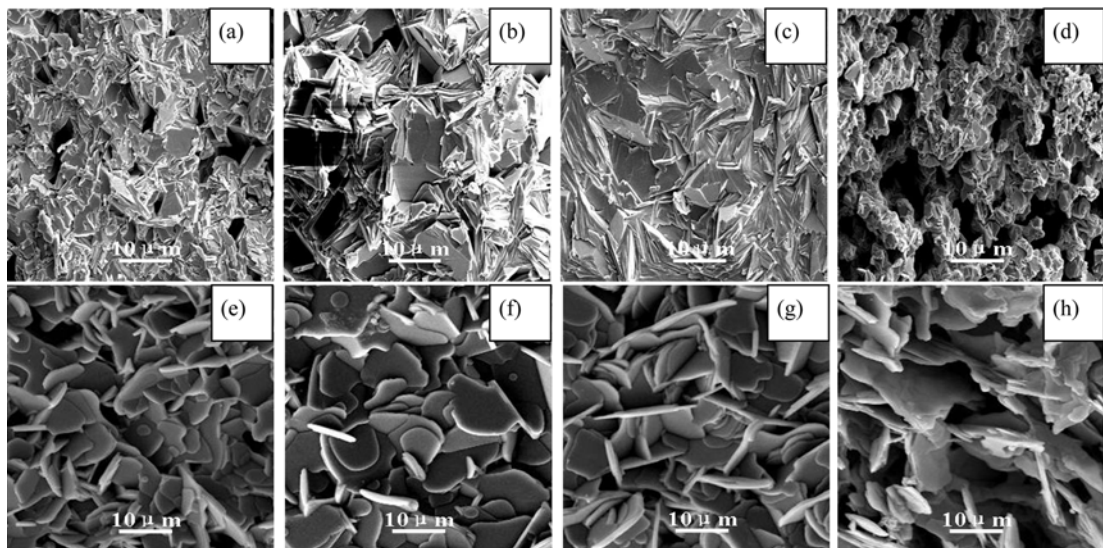


Fig. 4. Surface morphologies of the $\text{Ca}_{0.4}\text{Sr}_{0.6}\text{Bi}_4\text{Ti}_4\text{O}_{15}$ ceramics sintered at various temperatures.

(a) Sample A at 1100 °C, (b) Sample A at 1150 °C, (c) Sample A at 1180 °C, (d) Sample A at 1210 °C, (e) Sample B at 1100 °C (f) Sample B at 1150 °C (g) Sample B at 1180 °C (h) Sample B at 1210 °C.

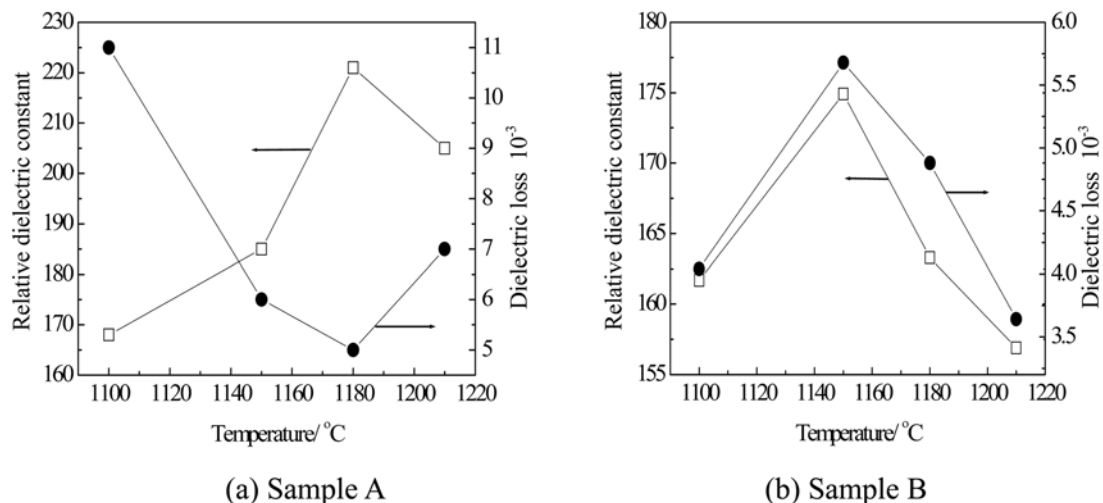


Fig. 5. Relative dielectric constant and dielectric loss of samples A and B sintered at various temperatures.

of a glass phase at high temperature. The results indicate that an appropriate increase of the sintering temperature is effective in improving the bulk density of $\text{Ca}_{0.4}\text{Sr}_{0.6}\text{Bi}_4\text{Ti}_4\text{O}_{15}$ ceramics.

Fig. 4 show the surface morphology of samples A and B sintered at various temperatures. In Fig. 4(a)-4(d), the reduction of porosity and growth of grains were observed which agreed well with the increase of the bulk density as described above. It can also be seen from Fig. 4(e)-4(h) that the density of sample B showed a similar tendency. Therefore, an appropriate increase of the sintering temperature can lead to an increase of bulk density as expected.

Fig. 5 shows the dielectric constant and dielectric loss of sample A and sample B at various sintering temperatures. The dielectric constant of the sample A initially increased with an increase in the sintering temperature up to 1180 °C and then decreased monotonically. The dielectric loss of

sample A and sample B showed the opposite tendency. When the sintering temperature was 1180 °C, it was noticeable that the values of the relative dielectric constants of sample A and sample B were 217.6 and 174.0, and the corresponding dielectric losses were 0.0027 and 0.005, respectively. The results showed that for the different cutting directions, the samples exhibited different dielectric behaviors.

The hysteresis loops of sample A and sample B sintered at 1180 °C for 2 h are shown in Fig. 6. It can be seen that sample A showed good ferroelectric properties with the measured P_r and E_c of 14.2 $\mu\text{C}/\text{cm}^2$ and 49.6 kV/cm, respectively, while the measured P_r and E_c for sample B were 7.9 $\mu\text{C}/\text{cm}^2$ and 33.5 kV/cm, indicating that the parallel cut sample showed better ferroelectric properties, which can be attributed to the higher degree of preferred orientation along the a -axis of the sample A [12-15]. These results were similar to those reported by Mao *et al* [9].

The ferroelectric properties of $\text{Ca}_{0.4}\text{Sr}_{0.6}\text{Bi}_4\text{Ti}_4\text{O}_{15}$ ceramics sintered at various temperatures are shown in Table 2. It can be seen that the P_r values increased at first and then decreased with an increase of the sintering temperature. The P_r reached a maximum value of 14.2 $\mu\text{C}/\text{cm}^2$ when the sintering temperature was 1180 °C, which was 79.7% larger than that of sample B. Compared with sample B, the coercive field of sample A was only slightly increased. It can also be seen that the remnant polarization reduced

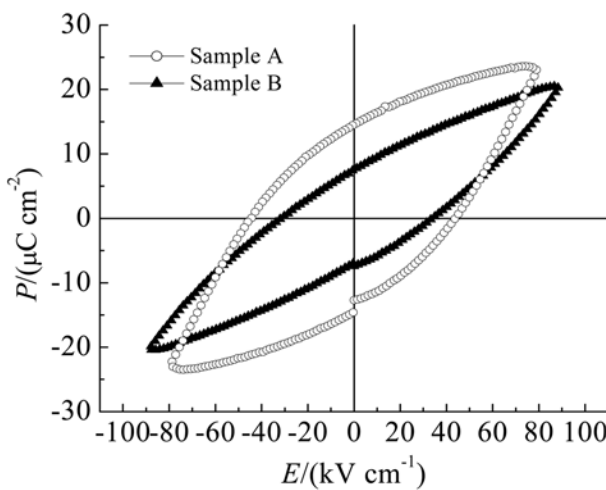


Fig. 6. Hysteresis loops of samples A and B sintered at 1180 °C for 2 h.

Table 2. Ferroelectric properties of the $\text{Ca}_{0.4}\text{Sr}_{0.6}\text{Bi}_4\text{Ti}_4\text{O}_{15}$ ceramics sintered at different temperatures

Sintering temperature/ °C	$P_r/(\mu\text{C}\cdot\text{cm}^{-2})$		$E_c/(\text{kV}\cdot\text{cm}^{-1})$	
	Sample A	Sample B	Sample A	Sample B
1100	4.2	1.1	22.3	16.0
1150	6.4	5.3	31.2	29.7
1180	14.2	7.9	49.6	33.5
1210	4.2	3.0	28.3	25.3

when the sintering temperature was 1210 °C. This may be attributed to the effects of the oxygen vacancies caused by the bismuth loss at high temperature [16].

Conclusions

1) $\text{Ca}_{0.4}\text{Sr}_{0.6}\text{Bi}_4\text{Ti}_4\text{O}_{15}$ ceramics with a -axis preferred orientation were prepared by a conventional solid-state method. The parallel cut sample showed a (200) preferred orientation, which may be attributed to the effects of the axial compression and highly anisotropic properties of the Bi-layered perovskite structure.

2) The sintering temperature had strong effects on the grain orientation and electrical properties of the $\text{Ca}_{0.4}\text{Sr}_{0.6}\text{Bi}_4\text{Ti}_4\text{O}_{15}$ ceramics. When the sintering temperature was 1180 °C, the sample A had the highest a -axis (200) orientation with a percentage of about 27.1%. Meanwhile, sample A also showed better dielectric properties with measured $\epsilon_r = 217.6$ and $\tan \delta = 0.0027$, respectively. The remnant polarization (P_r) of sample A was 14.2 $\mu\text{C}/\text{cm}^2$ with a coercive field $E_c = 49.6$ kV/cm. The results showed that for different cutting directions, the samples exhibited different electric behaviors.

Reference

- M.K. Jeon, H.J. Chung, K.W. Kim, K.S. Oh and S.I. Woo, Thin. Solid. Films. 498 (2005) 1-4.
- J.T. Zeng, Y.X. Li, D. Wang and Q.R. Yin, Solid. State. Commun. 133 (2005) 553-557.
- H. Lrie and M. Miyayama, Appl. Phys. Lett. 79[2] (2001) 251-253.
- Y. Noguchi, M. Miyayama and T. Kudo, Appl. Phys. Lett. 77[22] (2000) 3639-3641.
- M. Hirous, T. Suzuki, H. Oka, K. Itakura, Y. Miyauchi and T. Tsukada, Jpn. J. Appl. Phys. Part I. 38[9B] (1999) 5561-5563.
- E.C. Subbarao, Am. Ceram. Soc. 45[4] (1962) 166-169.
- S.H. Fan, J. Xu, GD. Hu and F.Q. Zhang, J. Chin. Ceram. Soc (in Chinese). 36[2] (2008) 100-103.
- X.Y. Mao and X.B. Chen, J. Chin. Ceram. Soc (in Chinese). 32[11] (2004) 1330-1334.
- X.Y. Mao, W. Wang, W. Wang and X.B. Chen, J. Chin. Ceram. Soc (in Chinese). 35[3] (2007) 312-316.
- C.J. Lu, Y. Qiao, Y.J. Qi, X.Q. Chen and J.S. Zhu, Appl. Phys. Lett. 87 (2005) 222901-222903.
- GD. Hu, S.H. Fan and X. Cheng, Jpn. J. Appl. Phys. 101 (2007) 054111-054116.
- J.F. Scott and C.A.P.D. Raujo, Science. 246 (1989) 1400-1406.
- B.H. Park, B.S. Kang, S.D. Bu, T.W. Noh, J. Lee and W. Jo, Nature. 401 (1999) 682-684.
- Y. Noguchi and M. Miyayama, Appl. Phys. Lett. 78[13] (2001) 1903-1905.
- Y. Masuda, H. Masumoto, A. Baba, T. Goto and T. Hirai, Jpn. J. Appl. Phys. 31 (1992) 3108-3112.
- F.Q. Zhang, S.H. Fan, J. Xu, GD. Hu, X.T. Yue, J. XU, and W. Zhang, J. Synth. Cryst. (in Chinese). 35[5] (2006) 1036-1040.